JOURNAL OF PROPULSION AND POWER
Vol. 18, No. 2, March–April 2002

Fuzzy Logic Intelligent System for Gas Turbine Module and System Fault Isolation

Ranjan Ganguli*
Indian Institute of Science, Bangalore 560012, India

A fuzzy logic intelligent system is developed for gas-turbine fault isolation. The gas path measurements used for fault isolation are exhaust gas temperature, low and high rotor speed, and fuel flow. These four measurements are also called the cockpit parameters and are typically found in almost all older and newer jet engines. The fuzzy logic system uses rules developed from a model of performance influence coefficients to isolate engine faults while accounting for uncertainty in gas path measurements. It automates the reasoning process of an experienced powerplant engineer. Tests with simulated data show that the fuzzy system isolates faults with an accuracy of 89% with only the four cockpit measurements. However, if additional pressure and temperature probes between the compressors and before the burner, which are often found in newer jet engines, are considered, the fault isolation accuracy rises to as high as 98%. In addition, the additional sensors are useful in keeping the fault isolation system robust as quality of the measured data deteriorates.

Nomenclature

$N1$	=	low rotor speed
$N2$	=	high rotor speed
$P25$	=	pressure between low-pressure compressor (LPC) and high-pressure compressor (HPC)
$P3$	=	pressure before burner
R	=	set of real numbers
T	=	set of terms
$T25$	=	temperature between LPC and HPC
$T3$	=	temperature before burner
U	=	universe of discourse of fuzzy set
x	=	element of fuzzy set
z	=	measurement deltas
Δ	=	change from baseline good engine
η	=	efficiency
$\mu_A(x)$	=	degree of membership of x in fuzzy set A
ξ	=	engine faults
σ	=	uncertainty as standard deviation
$\rightarrow$	=	mapping

Introduction

FAULT diagnosis has emerged as a key area of research in automation and intelligent systems.[1] Traditionally, fault diagnosis depended mainly on the experience of the operator. Because it is difficult for a human operator to react rapidly and consistently, there has been an effort to add "intelligence" to the fault diagnosis process. The model-based fault isolation approach, originating from control theory, has received increasing attention both in the research context and for real-world applications.[2–4] This approach involves defining residuals that differentiate the undamaged and the damaged system and then use of a mathematical model of the system, along with information processing methods, to extract information about the state of the system from the residuals. Such model-based approaches have been widely used for gas-turbine health monitoring.

Gas turbines are highly susceptible to damage because of a harsh aerothermodynamic environment and rapidly rotating blades. Gas-turbine performance diagnostics involves the accurate detection, isolation, and estimation of engine module performance, engine system problems, and instrumentation problems using measurements from the engine gas path. In performance diagnostics, discernable changes in gas path measurements from a baseline good engine are used to obtain changes in engine condition. Historically, the fault isolation problem was treated as a system identification problem and the analysis performed using Kalman filters.[5–13]

The use of Kalman filters for fault isolation and assessment in relative engine performance diagnostics started in the late 1970s and early 1980s, as shown in the works by Urban[5] and Volponi.[6] In these studies, the predictor–corrector property of the Kalman filter was used to predict engine module efficiencies, flow capacities, and areas, as well as sensor errors. Inputs to the Kalman filter were measurement deltas (deviations) from a baseline engine. Influence coefficients based on a linearized model were used to model engine performance, and noise properties of the system were captured using the measurement covariance matrix. Further details about the setup of the Kalman filter equations and the various matrices are discussed in Refs. 5 and 6.

In recent years, neural networks have also been applied to the gas-turbine fault detection and isolation problem. Whereas the Kalman filter literature focuses on long-term deterioration of the engine modules, the neural network literature focuses on single fault isolation.[14,15] Depold and Gass[14] found from a detailed study of airline engine maintenance records that a leading cause of reliability events such as in-flight shutdowns, delay and cancellations, or unscheduled engine removals is a single fault that immediately follows a rapid or step change in the engine gas path measurements. A power plant engineer observing the engine measurement data on a daily basis can detect such trend shifts. Because human beings performing routine tasks are prone to error, Depold and Gass have also investigated neural network methods for automated trend detection.[14]

Once a trend shift has been detected, the experienced powerplant engineer may be able to isolate the engine fault by consulting fingerprint charts provided by jet engine manufacturers. These fingerprint charts summarize the relationships between measurement deviations of gas path parameters from a baseline model and an engine fault and are developed using performance influence coefficients and a fault model. However, in reality, the powerplant engineers have frequent difficulty isolating the engine fault from gas path performance data. Powerplant engineers also look at other information such as engine maintenance history, trends from other engines on the same aircraft, borescope inspections, etc., to supplement information obtained from gas path signals. Even with all of these data

Received 5 June 2001; revision received 29 October 2001; accepted for publication 30 October 2001.

*Assistant Professor, Department of Aerospace Engineering. Member AIAA.

at their disposal, they have problems in accurately making a diagnosis. Part of this problem occurs because it is difficult to monitor manually large amounts of data as they become available after each flight. Therefore, automation of the knowledge base residing in the fingerprint charts allows the fault isolation to be performed as each measurement data point becomes available and may prevent expensive maintenance events. Recent studies have shown that once a trend change has been detected, a trained neural network can isolate the engine fault.[15]

The Kalman filter can also be configured to isolate engine single faults following a trend change, as shown in a recent study by Volponi et al. comparing the neural network and Kalman filter approaches.[16] Feedforward neural network architecture, along with backpropagation learning, was used to train the neural network using both ideal and noisy data. When the neural network is trained, it can isolate faults given a set of measurement deltas. For the single fault analysis, a bank of Kalman filters was used with each Kalman filter in the bank tuned to a particular engine fault. The Kalman filter with the least error was selected as being associated with the most likely fault. The engine faults used in this study were modeled using influence coefficients, and realistic noise was added to make the simulated data more realistic. The noise was obtained by taking an average of gas path measurement data from several different airlines for a given large commercial engine and is given in Ref. 15.

Typical gas path instrumentation measures exhaust gas temperature (EGT), low spool rotor speed $N1$, high spool rotor speed $N2$, and fuel flow (WF) at a given power condition. The four measurements are sometimes called the four basic parameters or cockpit parameters in gas-turbine performance diagnostics, and instrumentation to measure them is available in almost all older and newer engines. Some new engines have additional pressure and temperature instrumentation between the low-pressure and high-pressure compressor ($P25$ and $T25$) and before the burner ($P3$ and $T3$). The attempts to automate the engine performance diagnostics process can be viewed as an effort to add intelligence to these sensor measurements. Smart or intelligent systems have sensors and actuators and a controller or diagnostics system that acts as the brain of the smart system.[17] Such systems can report their current health condition and needed diagnostics automatically to the maintenance personnel. Smart systems for health monitoring are being increasingly suggested for expensive mechanical systems to prevent expensive downtime.

Most often, neural networks have been used for performing this function of automated reasoning. Neural networks are good at performing pattern recognition from noisy data. Most health monitoring problems can be posed as inverse problems where the objective is to extract the system state from the noisy measurements using a physics-based or data-based model. Neural networks are very powerful because they are universal function approximators.[18] However, neural networks often use backpropagation learning, which is computationally intensive. Kalman filters need considerable numerical linear algebra in the form of matrix inversions. Basically, for the single fault, the Kalman filter and neural network are being used in an attempt to automate the fingerprint charts. These fingerprint charts can be interpreted as rules, and rules can be used to define the knowledge based on an expert system. However, conventional expert systems have difficulty in handling uncertainty.[19]

Fuzzy expert systems are robust and are being increasingly used for health monitoring and other applications.[17,20] Recently, it has been proven that classical feedforward neural networks of the type used in engine diagnostics can be approximated to an arbitrary degree of accuracy by a fuzzy logic system, without having to go through the laborious training process needed by a neural network.[21] In addition, fuzzy rules follow human-language-based reasoning processes and are much easier to interpret and understand compared to neural networks that have a blackbox nature.[22] It is also possible to include heuristic knowledge from experts into a fuzzy logic system. In a recent work, Ganguli[23] showed that fuzzy logic systems could be used for engine module fault isolation under high levels of uncertainty. In this paper, we extend the fuzzy logic system to include system faults such as bleed leaks and failures and variable stator vane malfunctions, as well as certain instrumentation faults. In addition, fault isolation results from the fuzzy logic system are compared with results from neural networks and Kalman filter methods in the published literature.[16]

Module and System Faults

Typically, a twin-spool gas-turbine engine has five modules: fan (FAN), low-pressure compressor (LPC), high-pressure compressor (HPC), high-pressure turbine (HPT) and low-pressure turbine (LPT). The burner lies between the high-pressure compressor and the high-pressure turbine. The gas turbine operates by compressing the incoming air in the first three modules (FAN, LPC, and HPC), combusting the fuel–air mixture in the burner, and then expanding the air through the turbines (HPT and LPT) to generate power. Most damages to the engine manifest themselves as changes in either the module efficiency or flow capacity/area. The FAN, LPC, and HPC modules have flow capacities associated with them. The HPT and LPT modules have areas associated with them. Besides the five modules, the engine can experience system faults such as bleed leaks and failures, variable stator vane malfunctions, as well as certain instrumentation faults.[16] The fault models for the nine single faults considered in this study are shown in Table 1. Besides the five module faults, other faults considered are the start bleed leak (2.9 BLD), stability bleed leak (2.5 BLD), P49 indication problem (P49ER), and stator vane misrigging (HPCSVM). It is assumed that one and only one single fault occurs at a given time. The influence coefficients and fault models used to obtain the fingerprint charts are given by Volponi et al. and are used in this study.[16] The fingerprints for each of the nine faults are shown in Table 2. Figures 1 and 2 show an example of a fingerprint chart for the low-pressure turbine fault and 2.5 bleed fault, respectively. Figures 1 and 2 are obtained from the fingerprint charts in Table 2. From these charts, it appears that it would be difficult for a human engineer to look at several such charts and identify the correct fault from the measurement deltas. However, this task is well suited for a fuzzy logic system.

Table 1 Description and modeling of single faults

Fault	Description	Model
FAN	Damage in fan module	$-2\%\,\eta,\ -2.5\%$ FC
LPC	Damage in LPC module	$-2\%\,\eta,\ -2.2\%$ FC
HPC	Damage in HPC module	$-2\%\,\eta,\ -1.6\%$ FC
HPT	Damage in HPT module	$-2\%\,\eta,\ +1.5\%$ FP4
LPT	Damage in LPT module	$-2\%\,\eta,\ +3.3\%$ FP45
2.5 BLD	Stability bleed leak	2%
2.9 BLD	Start bleed leak	2%
HPCSVM	HPC stator vane misrigging	−6%
P49ER	$P49$ indication problem	2%

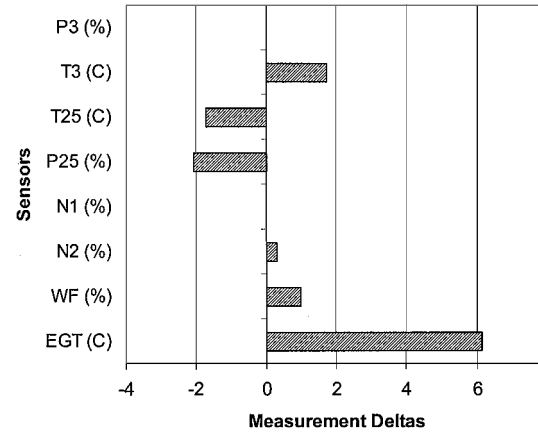

Fig. 1 Fingerprint chart for 2.5 bleed fault.

Table 2 Fingerprints for selected gas turbine faults

Measurement faults	ΔEGT, °C	ΔWF, %	Δ$N2$, %	Δ$N1$, %	Δ$P25$, %	Δ$T25$,°C	Δ$T3$,°C	Δ$P3$, %
FAN	13.60	1.60	−0.11	0.10	1.66	1.41	7.31	−0.34
LPC	21.77	2.58	−1.13	0.15	2.59	2.28	−8.05	−2.52
HPC	9.09	1.32	0.57	0.28	−2.35	−0.22	5.23	−0.01
HPT	2.38	−1.92	1.27	−1.96	−6.80	−6.90	2.84	−0.22
LPT	−7.72	−1.40	−0.59	1.35	3.99	3.91	3.15	0.05
2.5 bleed	6.15	0.99	0.31	0.01	−2.08	−1.71	1.73	0.01
2.9 bleed	8.43	2.12	0.58	0.12	−1.36	−1.27	−1.20	−0.04
HPCSVM	−5.71	−0.69	2.33	−0.02	−0.51	−0.54	2.05	0.54
P49ER	−0.65	−3.40	−0.49	−0.92	−1.11	0.03	−0.42	−2.44

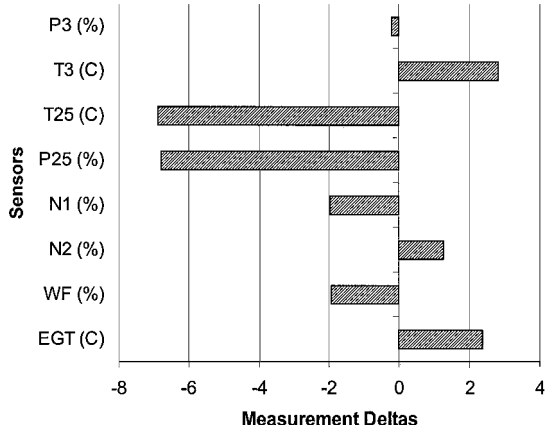

Fig. 2 Fingerprint chart for LPT fault.

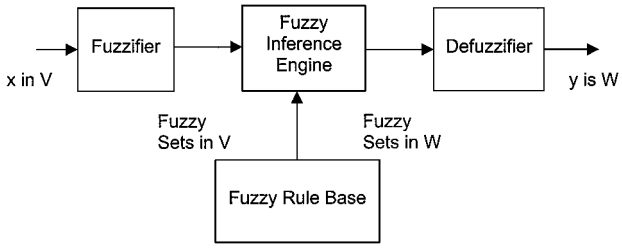

Fig. 3 Schematic representation of a fuzzy logic system.

Fuzzy Logic System

A fuzzy logic system (FLS) is a nonlinear mapping of an input feature vector into a scalar output.[24] Fuzzy set theory and fuzzy logic provide the framework for the nonlinear mapping. FLSs have been widely used in engineering applications because of the flexibility they offer designers and their ability to handle uncertainty. An FLS can be expressed as a linear combination of fuzzy basis functions and is a universal function approximater. Further information on FLSs is available from textbooks.[24]

A typical multi-input/single-output FLS performs a mapping from $V \in R^m$ to $W \in R$. Here,

$$f\colon V \in R^m \rightarrow W \in R$$

where

$$V = V_1 \times V_2 \times \cdots \times V_n \in R^m$$

is the input space and $W \in R$ is the output space.

A typical FLS maps crisp inputs to crisp outputs using four basic components: rules, fuzzifier, inference engine, and defuzzifier (Fig. 3). Once the rules driving the FLS have been fixed, the FLS can be expressed as a mapping of inputs to outputs.

Rules can come from experts or can be obtained from numerical data. In either case, engineering rules are expressed as a collection of IF–THEN statements such as IF u_1 is HIGH, and u_2 is LOW, THEN v is LOW. To formulate such a rule we need an understanding of 1) linguistic variables vs numerical values of a variable (e.g. HIGH vs 3.5%); 2) quantifying linguistic variables (e.g. u_1 may have a finite number of linguistic terms associated with it, ranging from NEGLIGIBLE to VERY HIGH), which is done using fuzzy membership functions; 3) logical connections between linguistic variables (e.g., AND, OR, etc.); and 4) implications such as IF A THEN B. We also need to understand how to combine more than one rule.

The fuzzifier maps crisp input numbers into fuzzy sets. It is needed to activate rules that are expressed in terms of linguistic variables. An inference engine of the FLS maps fuzzy sets to fuzzy sets and determines the way in which the fuzzy sets are combined. In several applications, crisp numbers are needed as an output of the FLS. In those cases, a defuzzifier is used to calculate crisp values from fuzzy values.

Fuzzy Sets

A fuzzy set F is defined on a universe of discourse U and is characterized by a degree of membership $\mu(x)$ that can take on values between 0 and 1. A fuzzy set generalized the concept of an ordinary set whose membership function only takes two values, zero and unity.

Linguistic Variables

A linguistic variable u is used to represent the numerical value x, where x is an element of U. A linguistic variable is usually decomposed into a set of terms $T(u)$, which cover its universe of discourse.[25]

Membership Functions

The most commonly used shapes for membership functions $\mu(x)$ are triangular, trapezoidal, piecewise linear, or Gaussian. The designer selects the type of membership function used. There is no requirement that membership functions overlap. However, one of the major strengths of fuzzy logic is that membership functions can overlap. FLS systems are robust and handle uncertainty well because decisions are distributed over more than one input class.[26] For convenience, membership functions are normalized to one so that they take values between 0 and 1 and thus define the fuzzy set.

Inference Engine

Rules for the fuzzy system can be expressed as

$$R_i\colon \text{IF } x_1 \text{ is } F_1 \text{ AND } x_2 \text{ is } F_2 \text{ AND } \cdots \text{AND } x_m \text{ is } F_m \text{ THEN } y = C_i, \quad i = 1, 2, 3, \ldots, M$$

where m and M are the number of input variables and rules, x_i and y are the input and output variables, and $F_i \in V_i$ and $C_i \in W$ are fuzzy sets characterized by membership functions $\mu_{F_i}(x)$ and $\mu_{C_i}(x)$, respectively. Each rule can be viewed as a fuzzy implication

$$F_{12\cdots m} = F_1 \times F_2 \times \cdots \times F_m \rightarrow C_i$$

which is a fuzzy set in $V \times W = V_1 \times V_2 \times \cdots \times V_m \times W$ with membership function given by

$$\mu_{R_i}(x, y) = \mu_{F_i}(x_1) * \mu_{F_2}(x_2) * \cdots * \mu_{F_m}(x_m) * \mu_{C_i}(y)$$

where the asterisk can be the min or product operator with $x = [x_1, x_2, \ldots, x_m] \in V$ and $y \in W$. This sort of rule covers many applications. The algebraic product is one of the most widely used T norms in applications and leads to product implication. In pattern recognition problems, the outputs are often crisp sets, and $\mu_{C_i}(y) = 1$ is often used for the product implication formula.[24]

Defuzzification

Popular defuzzification methods include maximum matching and centroid defuzzification.[27] Whereas centroid defuzzification is widely used for fuzzy control problems where a crisp output is needed, maximum matching is often used for pattern matching problems where we need to know the output class. Suppose there are K fuzzy rules and, among them, K_j rules ($j = 1, 2, \ldots, L$ and L is the number of classes) produce class C_j. Let D_p^i be the measurements of how the pth pattern matched the antecedent conditions (IF part) of the ith rule, which is given by the product of membership grades of the pattern in the regions that the ith rule occupies,

$$D_p^i = \prod_{i=1}^{m} \mu_{li}$$

where m is the number of inputs and μ_{li} is the degree of membership of measurement l in the fuzzy regions that the ith rule occupies. Let $D_p^{\max}(C_j)$ be the maximum matching degree of the rules (rules $j_l, l = 1, 2, \ldots, K_j$) generating class C_j,

$$D_p^{\max}(C_j) = \max_{l=1}^{K_j} D_p^{j_l}$$

then the system will output class C_{j*}, provided that

$$D_p^{\max}(C_{j*}) = \max_j D_p^{\max}(C_j)$$

If there are two or more classes that achieve the maximum matching degree, we will select the class that has the largest number of fired fuzzy rules. (A fired rule has a matching degree of greater than zero.)

Problem Formulation

Input and Output

Inputs to the FLS are measurement deltas and outputs are engine faults. We have eight measurements represented by z and nine engine faults represented by ξ. The objective is to find a functional mapping between z and ξ. Mathematically, this can represented as

$$\xi = F(z)$$

where

$$\xi = \{\text{FAN, LPC, HPC, HPT, LPT, 2.5 BLD, 2.9 BLD, HPCSVM, P49ER}\}^T$$

and

$$z = \{\Delta\text{EGT}, \Delta\text{WF}, \Delta N2, \Delta N1, \Delta P25, \Delta T25, \Delta P3, \Delta T3\}^T$$

Each measurement delta has uncertainty coming from both modeling errors and measurement errors, which makes the preceding inverse problem difficult to solve.

A schematic representation of the intelligent system for gas-turbine fault isolation is shown in Fig. 4. The gas turbine in its normal state of operation can be viewed as an input–output system operating in steady state. When a single fault occurs, there is a sharp change in the gas path sensor measurements reflecting the change in the gas turbine. This change in sensor measurement can then be compared to the baseline engine without faults to obtain a measurement residual. The residuals generated by the faulty system then

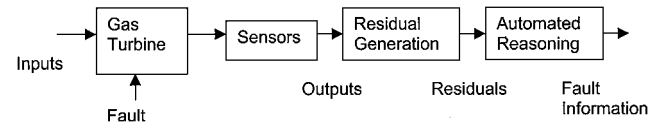

Fig. 4 Schematic representation of intelligent fault isolation system for gas turbine.

are subjected to automated reasoning by fuzzy logic to yield fault information.

Fuzzification

Here FAN, LPC, HPC, HPT, and LPT are fuzzy sets denoting the five engine modules. In addition, 2.5 BLD, 2.9 BLD, HPCSVM, and P49ER are fuzzy sets denoting the four system faults. Each fuzzy set has degrees of membership ranging from zero to one. In this paper, we are only interested in the isolating the fault and not in its magnitude. Therefore, we do not further decompose the module fuzzy sets using linguistic variables.

The measurement deltas ΔEGT, $\Delta N1$, $\Delta N2$, ΔWF, $\Delta P25$, $\Delta T25$, $\Delta T3$, and $\Delta P3$ are also treated as fuzzy variables. To get a high degree of resolution, they are further split into linguistic variables. For example, consider ΔEGT as a linguistic variable. It can be decomposed into a set of terms

$$T(\Delta\text{EGT}) = \{\text{Very High}-, \text{High}-, \text{Mediumhigh}-, \text{Medium}-, \text{Mediumlow}-, \text{Lowmedium}-, \text{Low}-, \text{Negligible}, \text{Low}+, \text{Lowmedium}+, \text{Mediumlow}+, \text{Medium}+, \text{Mediumhigh}+, \text{High}+, \text{Very High}+\}$$

where each term in $T(\Delta\text{EGT})$ is characterized by a fuzzy set in the universe of discourse $U(\Delta\text{EGT}) = \{-25^\circ\text{C}, 25^\circ\text{C}\}$, which is selected to include values spanning the fingerprint charts in Table 2, while maintaining symmetry. A total of 15 fuzzy sets are used to partition the numerical variables. It is found that a courser partition does not give very accurate results. A trial and error process and a careful study of the fingerprint charts were used to obtain the number of fuzzy sets. This process can be labeled heuristic reasoning.

The other seven measurement deltas are defined using the same set of terms as ΔEGT, spanning the following universes of discourse: $U(\Delta\text{WF}) = \{-4, 4\%\}$; $U(\Delta N2) = \{-3, 3\%\}$; $U(\Delta N1) = \{-3, 3\%\}$; $U(\Delta P25) = \{-6, 6\%\}$; $U(\Delta T25) = \{-10, 10^\circ\text{C}\}$; $U(\text{DT3}) = \{-10, 10^\circ\text{C}\}$; $U(\Delta P3) = \{-3, 3\%\}$. Because the influence coefficients on which the fingerprints are based represent a linear model, the diagnostic system should be limited to small measurement deltas.

Fuzzy sets with Gaussian membership functions are used. These fuzzy sets can be defined using the following equation:

$$\mu(x) = \exp\{-0.5[(x - m)/\sigma]^2\}$$

where m is the midpoint of the fuzzy set and σ is the uncertainty (standard deviation) associated with the variable. Table 3 gives the linguistic measure associated with each fuzzy set and the midpoint of the set for each measurement delta. The midpoints are selected to span the region ranging from a perfect engine (all measurement deltas are zero) to one with significant damage.

The fuzzy set corresponding to very high is defined slightly differently to account for the open-ended nature of the linguistic variable:

$$\mu(x) = \exp\{-0.5[(x - m)/\sigma]^2\} \qquad m_{\text{VH}-} < x \quad \text{OR} \quad x < m_{\text{VH}+}$$

$$\mu(x) = 1 \qquad m_{\text{VH}+} < x \quad \text{OR} \quad x < m_{\text{VH}-}$$

Here $m_{\text{VH}+}$ represents the midpoint corresponding to fuzzy set VH+. The standard deviations for the measurement deltas are representative of airline data[15] and are shown in Table 4. For illustration, Fig. 5 shows the membership functions for each of the 15 fuzzy

Table 3 Midpoints of Gaussian fuzzy sets

Linguistic measure	Symbol	Measurement deltas: ΔEGT, °C	ΔWF, %	ΔN1 and ΔN2, %	ΔP25, %	ΔT25 and ΔT3, °C	ΔP3, %
Very high−	VH−	−20	−3	−2	−6	−10	−3
High−	H−	−15	−2.5	−1.5	−4.5	−7.5	−2.5
Medium high−	MH−	−12.5	−2.25	−1.25	−3	−5	−2.25
Medium−	M+	−10	−2	−1	−2.5	−2.5	−1.5
Medium low−	ML−	−7.5	−1.5	−0.5	−2	−1.75	−0.75
Low medium−	LM−	−5	−1	−0.25	−1.5	−1.25	−0.5
Low−	L−	−2.5	−0.75	−0.125	−0.5	−0.25	−0.25
Negligible	N	0	0	0	0	0	0
Low+	L+	2.5	0.75	0.125	0.5	0.25	0.25
Low medium+	LM+	5	1	0.25	1.5	1.25	0.5
Medium low+	ML+	7.5	1.5	0.5	2	1.75	0.75
Medium+	M+	10	2	1	2.5	2.5	1.5
High+	H+	12.5	2.25	1.25	3	5	2.25
Medium high+	MH+	15	2.5	1.5	4.5	7.5	2.5
Very high+	VH+	20	3	2	6	10	3

Table 4 Measurement uncertainty

Measurement delta	Standard deviation
ΔEGT	4.23°C
ΔN1	0.25%
ΔN2	0.17%
ΔWF	0.50%
ΔP25	0.46%
ΔT25	1.12°C
ΔT3	1.99°C
ΔP3	0.24%

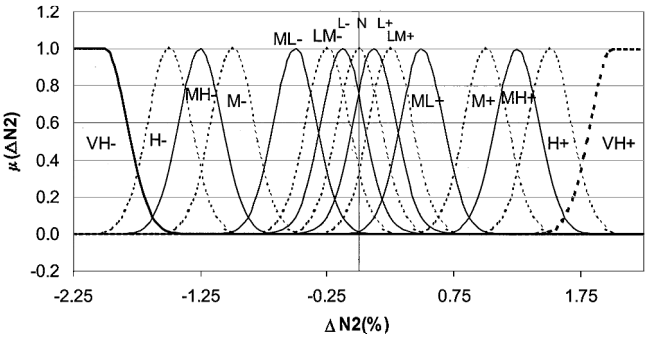

Fig. 5 Fuzzy sets for high rotor speed (*N*2) measurement delta.

sets for $\Delta N2$. The membership functions for the other fuzzy sets are similar in appearance. The midpoints for these fuzzy sets are obtained through heuristic reasoning.

Rules and Fault Isolation

Rules for the fuzzy system are obtained by fuzzification of the numerical values in the fingerprint charts using the following procedure[28,29]:

1) A set of eight measurement deltas corresponding to a given module fault is input to the FLS and the degree of membership of the elements of ΔEGT, ΔWF, $\Delta N2$, $\Delta N1$, $\Delta P25$, $\Delta T25$, $\Delta T3$, and $\Delta P3$ are obtained. Therefore, each measurement has 15 degrees of membership based on the linguistic measures in Table 3.

2) Each measurement delta is then assigned to the fuzzy set with the maximum degree of membership.

3) One rule is obtained for each fault by relating the measurement deltas with maximum degree of membership to a fault.

These rules are tabulated in Table 5. The linguistic symbols used in Table 5 are defined in Table 3. These rules can be read as follows for the FAN module:

IF

ΔEGT is Mediumlow− AND
ΔWF is Mediumlow− AND
$\Delta N2$ is Mediumlow− AND
$\Delta N1$ is Mediumhigh+ AND
$\Delta P25$ is High+ AND
$\Delta T25$ is Mediumhigh+ AND
$\Delta T3$ is Medium+ AND
$\Delta P3$ is Negligible

THEN

Problem in FAN module

The rules for the other faults can be similarly interpreted. These rules provide a knowledge base and represent how a human engineer would interpret data to isolate an engine fault using fingerprint charts. The fuzzy rules in Table 5 represent a fuzzified model of the fingerprints shown in Table 2. Because Gaussian fuzzy sets asymptotically approaching zero far from the midpoint are used, all of the rules fire at some level. For any given input set of measurement deltas, the fuzzy rules are applied using product implication. Once the fuzzy rules are applied for a given measurement, we have degrees of membership for each of the nine faults. For fault isolation, we are interested in the most likely fault. The fault with the highest degree of membership is selected as the most likely fault.

Results and Discussion

The fuzzy system is tested using simulated data developed from the fingerprint charts. For each fault, 1000 data sets are generated. Noise is added to the simulated measurement deltas using the typical standard deviations shown in Table 4. Testing with noisy data allows an analysis of the robustness of the system.

Table 6 shows the test results from the fuzzy system. The accuracy of fault detection is shown for the nine faults for four different sensor suites. Here, basic four refers to ΔEGT, ΔWF, $\Delta N1$, and $\Delta N2$ sensors only, which are present in almost all operational gas-turbine engines. The other results show the effect of addition of $P25$ and $T25$ sensors between the LPC and the HPC and $P3$ and $T3$ sensors before the burner. With the four basic measurements, the average success rate is about 89%. However, there is considerable variation is the fault isolation accuracy for the different faults. In particular, the bleed faults and the LPC are not isolated well. In these cases, the bleed faults are sometimes confused with the LPC and vice versa. The confusion between the LPC module fault and the bleed fault is because of the similarity in the directions of the fingerprints, which can be seen in the fuzzy rules. In the cases where the random error is high, the fingerprints for the LPC look very similar to those of the bleeds and vice versa.

Table 5 Rules for fuzzy system

Measurement faults	ΔEGT	ΔWF	Δ$N2$	Δ$N1$	Δ$P25$	Δ$T25$	Δ$T3$	Δ$P3$
HPC	MH+	ML+	L−	L+	LM+	LM+	H+	L−
HPT	VH+	H+	MH−	L+	M+	M+	H−	H−
LPC	M+	ML+	ML+	LM+	M−	L−	MH+	N
LPT	L+	M−	MH+	VH−	VH−	H−	M+	L−
FAN	ML−	ML−	ML−	MH+	H+	MH+	M+	N
2.5 bleed	LM+	LM+	LM+	N	ML−	ML−	ML+	N
2.9 bleed	ML+	MH+	ML+	L+	LM−	LM−	LM−	N
HPCSVM	LM−	L−	VH+	N	L−	L−	ML+	LM+
P49ER	N	VH−	ML−	M−	LM−	N	L−	H−

Table 6 Fault isolation results (%) from fuzzy system

Measurement faults	Basic four	Basic four +$P25$ +$T25$	Basic four +$P3$ +$T3$	All eight
HPC	92	100	98	100
HPT	100	100	100	100
LPC	82	85	94	94
LPT	100	100	100	100
FAN	100	100	100	100
2.5 bleed	69	78	82	89
2.9 bleed	61	93	94	99
HPCSVM	100	100	100	100
P49ER	100	100	100	100
Average success rate	89	95	96	98

Table 7 Comparison of fault isolation accuracy (%), neural network,[a] fuzzy system, and Kalman filter

Measurement faults	Basic four			All eight		
	Fuzzy	Neural	Kalman	Fuzzy	Neural	Kalman
HPC	92	90	100	100	100	100
HPT	100	100	100	100	100	100
LPC	82	90	90	94	60	90
LPT	100	100	100	100	100	100
FAN	100	100	100	100	100	100
2.5 bleed	69	75	50	89	80	85
2.9 bleed	61	87	80	99	87	97
HPCSVM	100	100	100	100	100	100
P49ER	100	100	100	100	100	100
Average success rate	89	93	91	98	91	97

[a]Neural network and Kalman filter results are from Ref. (16).

Placing additional sensors to measure $P25$ and $T25$ results in the fault isolation accuracy increasing from 86 to 95%. There is a marked increase in the isolation accuracy for the 2.5 and 2.9 bleed faults. In case additional sensors besides the basic four were used to measure $P3$ and $T3$, the average fault isolation accuracy increases from 89 to 96%. In particular, the isolation accuracy increased from 82 to 94% for the LPC fault. In addition, there is also an increase in the isolation accuracy for the 2.5 and 2.9 bleed faults. Placing the $T3$ and $P3$ sensors results in a greater improvement in fault isolation accuracy than the $T25$ and $P25$ sensors. However, when all of the eight sensors (basic $4 + P25 + T25 + T3 + P3$) are used, the average fault isolation accuracy rises to 98%.

Table 7 compares results obtained using the fuzzy logic system with those obtained using neural network and Kalman filters in Ref. 16. The same test cases were used for these results. There is a close agreement between the results. The fuzzy system and the Kalman filter give better results with the eight-sensor suite, compared to the neural network. This may be because the fuzzy system and the Kalman filter include the knowledge of the fingerprint charts in their rule base and influence coefficient matrix, respectively, whereas the neural network has to learn the relationships from the simulated training data. Volponi et al.[16] have given a detailed discussion on why the nonlinear multiplayer perceptron neural network gives better results with four measurements than with eight

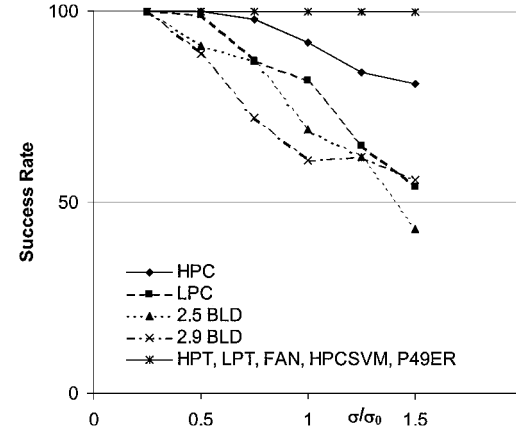

Fig. 6 Fault isolation success rate with increasing uncertainty in data (basic four measurements only).

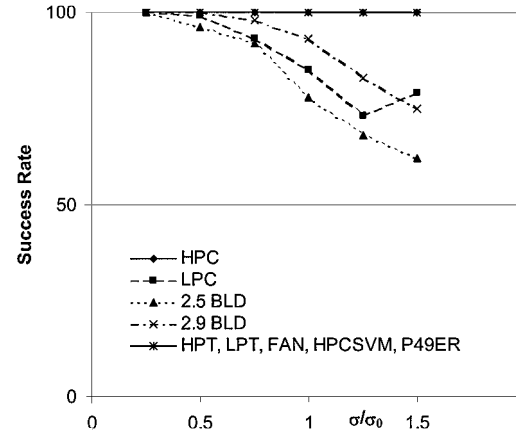

Fig. 7 Fault isolation success rate with increasing uncertainty in data (basic four measurements +$P25$ + $T25$).

measurements. The key problems appear to be that the neural networks learn the model from noisy data and have a high degree of distributed nonlinearity.

The results discussed until now were obtained for test data generated using standard deviations given in Table 4 and that were also used in creating the membership functions for the FLS. Figures 6–10 show results obtained for the FLS for test data generated for various levels of uncertainty. Here σ_0 is the baseline standard deviation given in Table 4. Results are obtained for uncertainty ranging from 25% of the baseline value to 150% of the baseline value. Figure 6 shows the influence of measurement uncertainty for a system with only the four basic parameters. For very low uncertainty levels ($\sigma/\sigma_0 = 0.25$) the FLS shows 100% accuracy in fault isolation. As the measurement data deteriorate, the fault isolation success rate falls for the HPC, LPC, 2.5 bleed, and 2.9 bleed faults. The turbine and fan modules and HPCSVM and P49ER faults are isolated with 100% accuracy even with low-quality data.

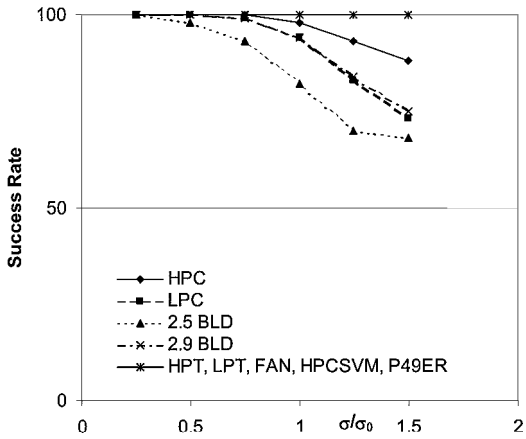

Fig. 8 Fault isolation success rate with increasing uncertainty in data (basic four measurements +$T3$ + $P3$).

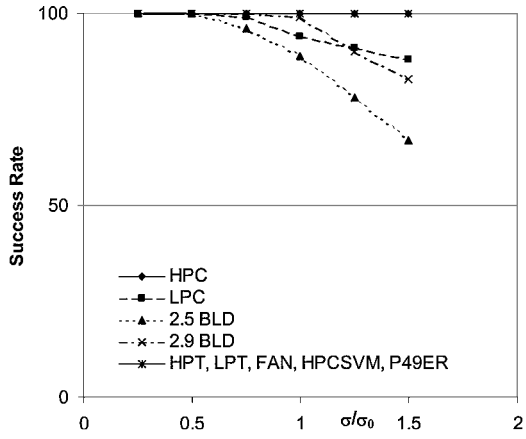

Fig. 9 Fault isolation success rate with increasing uncertainty in data (all eight measurements).

The inclusion of $P25$ and $T25$ sensors results in some improvement in the fault isolation accuracy, as shown in Fig. 7. Similarly, the inclusion of $P3$ and $T3$ sensors over and above the basic four results in some improvement in accuracy, as shown in Fig. 8. Finally, inclusion of all eight sensors shows considerable improvement in fault isolation accuracy, as shown in Fig. 9. For uncertainty levels lower than σ_0, the fault isolation accuracy is significantly improved. Thus, it is very important to focus on data cleaning and rectification methods, as well as improved sensors to remove potential outliers in the data.[30] In addition, the robust nature of the FLS is clear from the fault isolation accuracy deteriorating gradually as uncertainty levels increase.

Finally, the average success rates for the four different measurement suites are summarized in Fig. 10. Note that the importance of having the additional sensors becomes more important as data quality falls. The FLS is able to identify the correct fault despite the presence of considerable uncertainty in the measurements.

The current study demonstrated the effectiveness of the fuzzy logic approach in the isolation of single faults following a sharp trend change. However, the study makes several assumptions and simplifications:

1) Unmodeled single faults, sensor faults and multiple faults are not addressed.

2) Only module faults are considered, and pure combustor performance problems are neglected.

3) The relationships between the module efficiencies and flow capacities/areas are considered fixed at the values provided by engine manufacturers.

4) The robustness of the system to noise in the measured data is analyzed by scaling all of the uncertainties to the same factor. The effect of scaling the uncertainty individually per measurement is neglected.

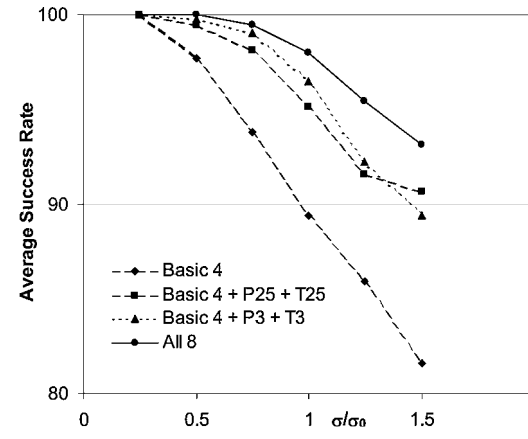

Fig. 10 Comparison of average fault isolation success rate for different sensor suites and uncertainty in data.

5) Missing measurements are not considered.

6) A "winner take all" approach is used to find the most likely fault, and the possibility of using "beliefs" from the output of the system to study the possible confounding between the first and second most likely faults is not considered.

These issues need to be addressed in future research work to make the diagnostic system more useful for real-world gas-turbine health monitoring.

Conclusions

An FLS is developed for gas-turbine engine performance diagnostics. It takes measurement deviations from a baseline model of a good engine and isolates the engine fault. The FLS operates with four basic (cockpit) measurements (EGT, WF, $N1$, and $N2$) and analyzes deterioration in five modules (FAN, LPC, HPC, HPT, and LPT) and four system faults (2.5 bleed, 2.9 bleed, HPCSVM, $P49$Error). These measurements are available on most jet engines. The FLS is based on fingerprint charts provided by engine manufacturers and widely used by airline engineers.

Results show that the FLS has a success rate of about 90% in isolating the faulty engine module with four cockpit measurements. In cases where the FLS is confounded, it was due to large uncertainty in the data. The FLS, therefore, can be used as a robust expert system for automating the process of interpreting gas-turbine performance fingerprint charts.

Additional pressure and temperature sensors between the compressors ($P25$ and $T25$) or before the burner ($P3$ and $T3$) improve the fault isolation accuracy to about 95%. When all eight sensors are used together, the FLS shows an accuracy of 98% in fault isolation. Additional sensors become more important as data quality deteriorates. Therefore, additional sensors besides the four cockpit sensors are useful and recommended for accurate and robust fault isolation.

References

[1]Patton, R. J., Frank, P. M., and Clark, R. N., *Fault Diagnosis in Dynamic Systems: Theory and Applications*, Prentice–Hall, London, 1989.

[2]Frank, P. M., "Fault Diagnosis in Dynamic Systems Using Analytical and Knowledge Based Redundancy—A Survey and Some New Results," *Automatica*, Vol. 26, No. 6, 1990, pp. 459–474.

[3]Dexter, A. L., "Fuzzy Model Based Fault Diagnosis," *IEE Proceedings on Control Theory Applications*, Vol. 142, No. 6, 1995, pp. 545–550.

[4]Isermann, R., "Supervision, Fault-Isolation and Fault Diagnosis Methods—An Introduction," *IFAC Journal: Control Engineering Practice*, Vol. 5, No. 5, 1997, pp. 639–652.

[5]Urban, L. A., "Gas Path Analysis Applied to Turbine Engine Conditioning Monitoring," AIAA Paper 72-1082, Dec. 1972.

[6]Volponi, A., "Gas Path Analysis: An Approach to Engine Diagnostics, Time-Dependent Failure Mechanisms and Assessment Methodologies," Cambridge Univ. Press, Cambridge, England, U.K., 1983.

[7]Doel, D. L., "TEMPER—A Gas Path Analysis Tool for Commercial Jet Engines," *ASME Journal of Engineering for Gas Turbines and Power*, Vol. 116, 1994, pp. 82–89.

[8]Gallops, G. W., Bushman, M. A., and Gallops, G. W., "In-Flight Performance Diagnostic Capability of an Adaptive Engine Model," AIAA Paper 92-3746, July 1992.

[9]Kerr, L. J., Nemec, T. S., and Gallops, G. W., "Real-Time Estimation of Gas Turbine Engine Damage Using a Control Based Kalman Filter Algorithm," American Society of Mechanical Engineers, ASME Paper 91-GT-216, 1991.

[10]Merrington, G. L., "Fault Diagnosis in Gas Turbines Using a Model Based Technique," American Society of Mechanical Engineers, ASME Paper 93-GT-13, 1993.

[11]Stamatis, A., Mathioudakis, K., Berios, K., and Papailiou, K. D., "Jet Engine Fault Detection with Differential Gas Path Analysis at Discrete Operating Points," *Journal of Propulsion and Power*, Vol. 7, No. 6, 1991, pp. 1043–1048.

[12]Luppold, R. H., Roman, J. R., Gallops, G. W., and Kerr, L. J., "Estimating In-Flight Engine Performance Variations Using Kalman Filter Concepts," AIAA Paper 89-2584, July 1989.

[13]Volponi, A. J., and Urban, L. A., "Mathematical Methods of Relative Engine Performance Diagnostics," Society of Automotive Engineers Transactions, Vol. 101, *Journal of Aerospace*, 1992.

[14]DePold, H., and Gass, F. D., "The Application of Expert Systems and Neural Networks to Gas Turbine Prognostics and Diagnostics," *Journal of Engineering for Gas Turbine and Power*, Vol. 121, No. 4, 1999, pp. 607–612.

[15]Lu, P. J., Hsu, T. C., Zhang, M. C., and Zhang, J., "An Evaluation of Engine Fault Diagnostics Using Artificial Neural Networks," *Journal of Engineering for Gas Turbine and Power*, Vol. 123, No. 2, 2001, pp. 240–246.

[16]Volponi, A. J., Depold, H., Ganguli, R., and Daguang, C., "The Use of Kalman Filter and Neural Network Methodologies in Gas Turbine Performance Diagnostics: A Comparative Study," American Society of Mechanical Engineers, ASME Paper 00-GT-547, 2000.

[17]Sinha, N. K., and Gupta, M. M., *Soft Computing and Intelligent Systems: Theory and Applications*, Academic Press, San Diego, 2000.

[18]Hornik, K., Stinchcombe, M., and White, H., "Multilayer Feedforward Networks are Uniform Approximators," *Neural Networks*, Vol. 2, No. 3, 1989, pp. 369–366.

[19]Luger, G. F., and Stubblefield, W. A., *Artificial Intelligence—Structures and Strategies for Complex Problem Solving*, Addison Wesley Longman, Reading, MA, 1998.

[20]Yen, J., Laqngani, R., and Zadeh, L. A. (eds.), *Industrial Applications of Fuzzy Logic and Intelligent Systems*, IEEE Press, New York, 1995.

[21]Hong, X. L., and Chen, P. C. L., "The Equivalence Between Fuzzy Logic Systems and Feedforward Neural Networks," *IEEE Transactions on Neural Networks*, Vol. 11, No. 2, 2000, pp. 356–365.

[22]Zadeh, L. A., "Fuzzy Logic = Computing with Words," *IEEE Transactions on Fuzzy Systems*, Vol. 4, No. 2, 1996, pp. 103–101.

[23]Ganguli, R., "Application of Fuzzy Logic for Fault Isolation of Jet Engines," American Society of Mechanical Engineers, ASME Paper 01-GT-13.

[24]Kosko, B., *Fuzzy Engineering*, Prentice–Hall, Upper Saddle River, NJ, 1997.

[25]Zadeh, L. A., "The Concept of a Linguistic Variable and Its Application to Approximate Reasoning," *Information Sciences*, Vol. 8, No. 2, 1975, pp. 199–251.

[26]Mengali, G., "The Use of Fuzzy Logic in Adaptive Flight Control Systems," *Aeronautical Journal*, Vol. 104, No. 1031, 2000, pp. 31–37.

[27]Chi, Z., and Yan, H., "ID3 Derived Fuzzy Rules and Optimized Defuzzification for Handwritten Character Recognition," *IEEE Transactions on Fuzzy Systems*, Vol. 4, No. 1, 1993, pp. 24–31.

[28]Abe, S., and Lan, M. S., "A Method for Fuzzy Rules Extraction Directly from Numerical Data and Its Application to Pattern Recognition," *IEEE Transactions on Fuzzy Systems*, Vol. 3, No. 1, 1995, pp. 18–28.

[29]Wang, L. X., and Mendel, J. M., "Generating Fuzzy Rules by Learning from Examples," *IEEE Transactions on Systems, Man and Cybernetics*, Vol. 22, No. 6, 1992, pp. 1414–1427.

[30]Ganguli, R., "Data Rectification and Detection of Trend Shifts in Jet Engine Gas Path Measurements Using Median Filters and Fuzzy Logic," American Society of Mechanical Engineers, ASME Paper 01-GT-14.